

Rare-earth Sm-Co nanopowder prepared by low oxygen-induction thermal plasma process

K. Park^{1,2}, Y. Hirayama², M. Shigeta³, Z. Liu⁴, M. Kobashi¹ and K. Takagi²

¹Department of Materials Process Engineering, Nagoya University, Aichi, Japan

²Magnetic Powder Metallurgy Research Center, National Institute of Advanced Industrial Science and Technology (AIST), Aichi, Japan

³Department of Mechanical Systems Engineering, Tohoku University, Miyagi, Japan

⁴Innovative Functional Materials Research Institute, National Institute of Advanced Industrial Science and Technology (AIST), Aichi, Japan

Abstract: The rare-earth Sm-Co alloy nanopowder was successfully prepared by the low oxygen-induction thermal plasma (LO-ITP) process. The hard magnetic compounds of SmCo₅ and SmCo₇ were identified by the X-ray diffraction (XRD) profile. In addition, the unique core/shell particle with a Co-core/Sm-Co-shell structure was found by microstructure analysis. The particle formation mechanism of the Sm-Co alloy particles and core/shell particles was numerically demonstrated.

Keywords: Sm-Co alloy, induction thermal plasma, permanent magnet, nanoparticles

1. Introduction

Fine rare-earth (RE) alloy particles that have anisotropic magnetic behavior and high coercivity could be an optimal raw material for a high-performance permanent magnet. This RE magnetic raw powder that meets both requirements can be achieved by particle size refinement [1]. The thermal plasma process is a promising method to prepare single crystal nanoparticles with a smaller average particle diameter of 100 nm [2-4]. An important point is to avoid oxidation when handling metal nanopowders. Recently, we developed a new technique called the low oxygen-induction thermal plasma (LO-ITP) process which makes it possible to handle the prepared nanopowder in a low oxygen atmosphere with an oxygen level below about 0.5 ppm [5-7]. In this study, the Sm-Co alloy was selected to demonstrate the effectiveness of the LO-ITP process in preparing a RE alloy nanopowder. A detailed phase and microstructure analysis of Sm-Co nanopowder was intensively conducted. In addition, the numerical calculations revealed the particle formation mechanism of the Sm-Co nanopowder.

2. Experimental procedure

Sm ($D_{90} = 18 \mu\text{m}$, Sinfonia Technology Co., Ltd., Japan) and Co ($D_{90} = 8 \mu\text{m}$, Kojundo Chemical Lab. Co., Ltd., Japan) powders were used as the starting materials. These two raw powders were mixed at an atomic ratio of Sm:Co = 1:5. The ITP was generated using a RF generator (TP-40020NPS, JEOL Ltd.) with a power of 6 kW and a frequency of 13.56 MHz. G1 grade Ar gas (purity 99.99995%) was used as the plasma gas with a flow rate of 35 L/min and powder feeding gas with a flow rate of 3 L/min using a powder feeding system (TP-99010FDR, JEOL Ltd.). The mixture of Sm and Co powder was introduced from the top of the thermal plasma by the powder feeder for 10 min. The processed powder was

collected from the chamber and handled in a glovebox with an oxygen level below 0.5 ppm [7].

The particle morphologies and size distribution were estimated from images acquired by field emission-scanning electron microscope (FE-SEM, JSM-7800F, JEOL Ltd). The phases were identified using a X-ray diffractometer (XRD) with a wavelength of 0.08856 nm at the BL5S2 beamline of the Aichi Synchrotron Radiation Center. The crystal structure and phases were investigated with a transmission electron microscope (TEM, JEMARM200CF, JEOL Ltd.). The detailed numerical model description has been described elsewhere [7].

3. Results

Fig. 1a shows an SEM image of the Sm-Co nanopowder. The nanopowder with a relative sphere morphology was obtained. In Fig. 1b, the histogram of particle size distribution was made using 300 randomly selected particles in Fig. 1a. The mean particle diameter of 61 nm and standard deviation of 20 nm were estimated by fitting the log-normal distribution function.

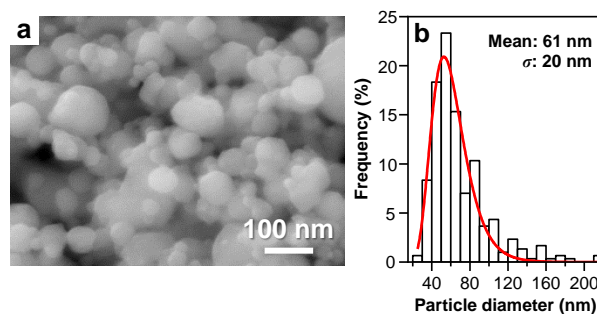


Fig. 1. a) SEM image and b) particle size distribution of the Sm-Co nanopowder. The red linear curve was fitted by the log-normal distribution function.

Fig. 2 shows the XRD profile with the calculated XRD patterns obtained by Rietveld refinement of the Sm-Co

nanopowder. The peaks of hard magnetic compounds, CaCu_5 type- SmCo_5 and TbCu_7 type- SmCo_7 , were identified. According to the Rietveld refinement, the amounts of the achieved hard magnetic compounds SmCo_7 and SmCo_5 phases were estimated as 52.4 wt% and 28.1 wt%, respectively.

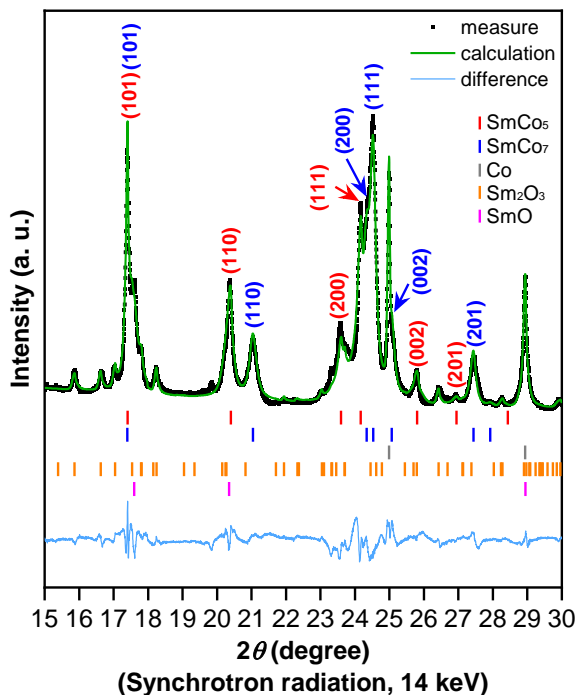


Fig. 2. XRD profile and result of Rietveld refinement of the Sm-Co nanopowder.

Fig. 3a shows a high-angle annular dark field (HAADF)-STEM image and elemental mapping images of the Sm-Co nanopowder. It was observed that the composition ratio of Sm and Co was constant within each particle. According to the energy dispersive X-ray spectroscopy (EDS) analysis, the compositions of particles #1 and #2 were $\text{Sm}:\text{Co} = 10.8:89.2$ and $15.9:84.1$ (at%), respectively. The possible Sm-Co alloy phases were the SmCo_7 phase or the $\text{Sm}_2\text{Co}_{17}$ phase or even a mixture of these phases for particle #1 and the SmCo_5 phase for particle #2. These results are consistent with the results obtained from the XRD measurement.

Fig. 3b shows HAADF-STEM images of the core/shell particle. The diameter of this core/shell particle was measured as about 192 nm, and the core diameter and shell thickness were estimated to be 84 nm and 50 nm, respectively. According to the elemental mapping of Sm, Co, and their overlay, the core comprises of Co without Sm, while the shell comprises Sm-Co alloy. Oxide phases were not identified at the interface of the core and shell, indicating that a sharp oxide-free interface between the core and the shell was obtained.

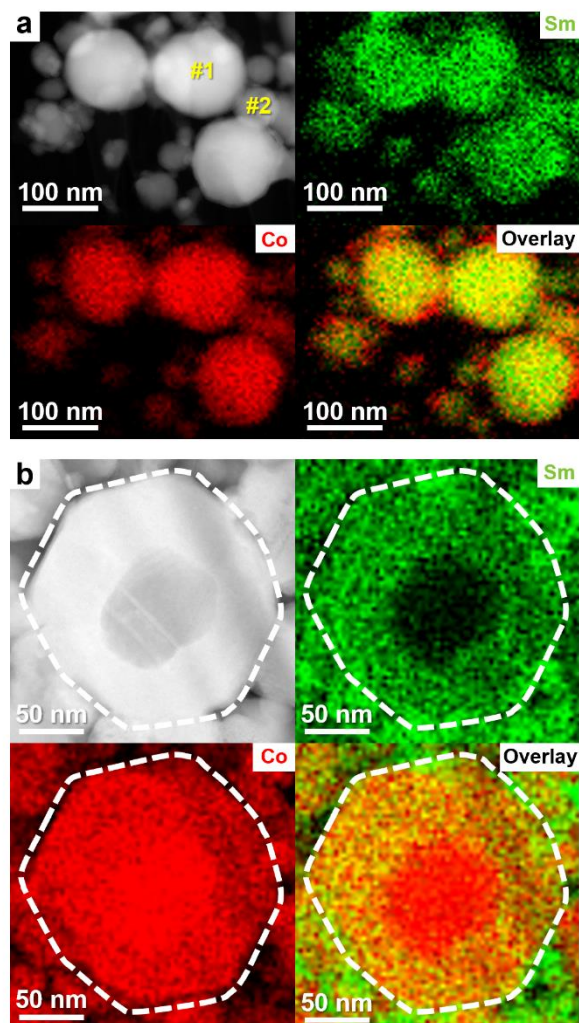


Fig. 3. HAADF-STEM image and elemental mapping images of a) the Sm-Co alloy nanoparticles and b) Co-core/Sm-Co-shell structural particle.

To obtain a detailed understanding of the formation mechanism of alloy and core/shell particles in the thermal plasma process, a numerical analysis using a binary aerosol formation-growth model was carried out [7]. Fig. 4a-c show the numerically obtained snapshots of the size-composition distributions of the particles during the growth process at 1585, 1400, and 1100 K. The gray and white areas on Fig. 4a-c background indicate solid and liquid areas of the particles, respectively. The particles produced at the corresponding temperatures are portrayed in the inset schematic illustrations. Fig. 4d shows the conversion ratio from the contributions of homogeneous nucleation and heterogeneous condensation.

At 1585 K, the majority of the particles were created as liquid Sm-Co droplets with condensed Sm and Co as shown in Fig. 4a since vapor molecules of Sm and Co simultaneously condensed on both solid large particles and liquid small particles, as indicated in Fig. 4d. At 1400 K, almost all particles were solidified, as shown in Fig. 4b. In Fig. 4d, the conversion ratio of Sm is 30%, indicating that

Sm molecules were still in the vapor phase and would condense on the solid particles which had already formed. Thus, the solid Sm-Co particles were covered with thick condensed Sm at this temperature. At 1100 K, condensation of Sm was completed, as indicated in Fig. 4d, and all the particles were solid in Fig. 4c. At temperatures below 1100 K, at which condensation of both Sm and Co was complete, as shown in Fig. 4d, 90% of the particles were Sm-Co-core/Sm-shell particles and 10% were Sm-Co alloy particles as the final products. Therefore, numerical analysis is of great help in predicting the complex particle formation mechanism of elements with very different intrinsic properties such as surface tension and vapor pressure. However, the number of core/shell particles observed by TEM was much smaller than that of alloy particles. The one possible reason for this contradiction is that the calculations did not consider the diffusion of atoms in the particles. Experimentally, most particles formed the Sm-Co alloy, and only a small number of core/shell particles in which atomic diffusion was insufficient were created.

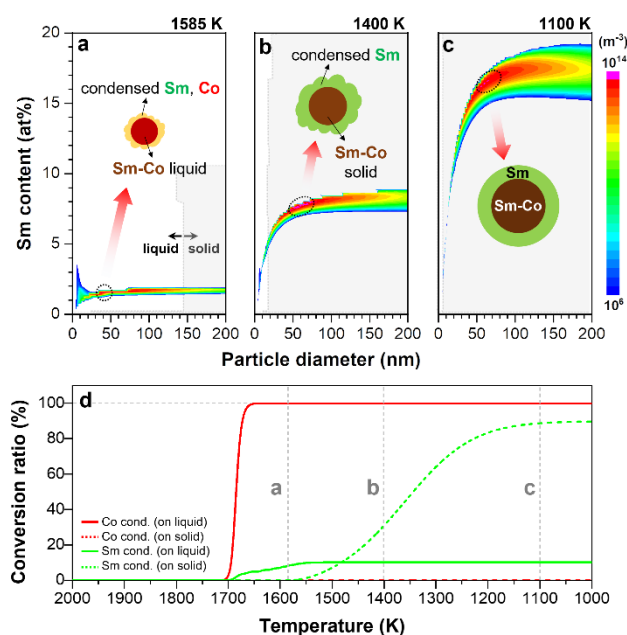


Fig. 4. Particle size-composition distribution of Sm-Co particles at a) 1585 K, b) 1400 K and c) 1100 K. d) Conversion ratio in a Sm-Co system.

4. Conclusion

The RE Sm-Co alloy nanoparticles with a mean particle diameter of 61 nm were successfully prepared by the LO-ITP process. The hard magnetic compounds SmCo_5 and SmCo_7 were obtained without oxidation. The unique Co-core/Sm-Co-shell structural particle was identified by STEM observation. This Co-core/Sm-Co-shell particle has an ideal microstructure that could behave as a nanocomposite magnet powder. In addition, the particle formation mechanism of the Sm-Co alloy particles and core/shell particles was demonstrated by the numerical analysis. This study strongly suggested that the LO-ITP

process is a promising new strategy for preparing RE alloy nanopowders.

Acknowledgements

The figures in this abstract were reprinted from Journal of Alloys and Compounds, vol. 882, K. Park *et al.*, Anisotropic Sm-Co nanopowder prepared by induction thermal plasma, 2021, with permission from Elsevier.

5. References

- [1] J.S. Lee, J.M. Cha, H.Y. Yoon, J.K. Lee, Y.K. Kim, *Sci. Rep.*, **5**, 1 (2015).
- [2] M. Shigeta, A.B. Murphy, *J. Phys. D Appl. Phys.*, **44**, 174025 (2011)
- [3] K. Kim, T. Kim, *J. Appl. Phys.*, **125**, 070901 (2019)
- [4] J.H. Seo, B.G. Hong, *Nucl. Eng. Technol.*, **44**, 9 (2012)
- [5] Y. Hirayama, K. Suzuki, W. Yamaguchi, K. Takagi, *J. Alloy. Compd.*, **768**, 608 (2018)
- [6] Y. Hirayama, K. Takagi, *J. Alloy. Compd.*, **792**, 594 (2019)
- [7] K. Park, Y. Hirayama, M. Shigeta, Z. Liu, M. Kobashi, K. Takagi, *J. Alloys Compd.*, **882**, 160633 (2021)